JCZ: Zoologischer Anzeiger - A Journal of Comparative Zoology 323 (2026) 89–99

Contents lists available at ScienceDirect

Zoologischer Anzeiger

journal homepage: www.elsevier.com/locate/jcz

Comparative analysis of skull morphology in the Sumatran rhinoceros of Borneo (*Dicerorhinus sumatrensis harrissoni*)

Danang Dwi Cahyadi [a], Deanty Chairunnisa [a], Supratikno [a], Savitri Novelina [a], Chairun Nisa' [a], Srihadi Agungpriyono [a], Dedi Chandra [b], Kurnia Oktavia Khairani [c], Zulfiqri [c], Muhammad Agil [d], Jono Adiputro [e], Matheas Ari Wibawanto [f], Nurhidayat [a,*]

[a] Division of Anatomy Histology and Embryology, School of Veterinary Medicine and Biomedical Sciences, IPB University, Bogor, West Java, 16680, Indonesia
[b] Directorate of Species and Genetic Conservation, Directorate General of Conservation of Natural Resources and Ecosystem, Ministry of Forestry, Jakarta, 10270, Indonesia
[c] Aliansi Lestari Rimba Terpadu (ALeRT), Bogor, West Java, 16151, Indonesia
[d] Division of Reproduction and Obstetrics, School of Veterinary Medicine and Biomedical Sciences, IPB University, Bogor, West Java, 16680, Indonesia
[e] Kelian Rhino Sanctuary, West Kutai, East Kalimantan, Indonesia
[f] The Natural Resources Conservation Agency (BKSDA), Samarinda, East Kalimantan, 75243, Indonesia

ARTICLE INFO

Handling Editor: Janine M Ziermann

Keywords:
Cranial capacity
Cranium
Sumatran rhinoceros
Endangered fauna
Skeleton

ABSTRACT

The Bornean population of the Sumatran rhinoceros (*Dicerorhinus sumatrensis harrissoni*) has been geographically and genetically isolated from its Sumatran counterpart (*D. s. sumatrensis*) for thousands of years, yet the extent of their morphological divergence remains poorly understood. This study provides the first detailed comparative analysis of cranial skeletal structures in the Bornean Sumatran rhinoceros, using the female specimen Najaq, and evaluates its anatomical distinctions from the Sumatran subspecies. Additional morphometric data available from previous studies were used for comparison. Our findings reveal significant morphological differences, with the Bornean subspecies exhibiting smaller cranial size, compared to those of the Sumatran subspecies, as indicated by the basal length, occipitonasal length, and zygomatic breadth. The Sumatran rhinoceros exhibited an acute occipital angle, which was sharper in the Sumatran subspecies (~70°) than that of the Bornean subspecies (75°). Additionally, a second pair of upper incisors was noted in the Najaq specimen, an abnormality that rarely occurs in rhinoceroses. These structural variations suggest adaptive or evolutionary divergence, potentially driven by long-term geographic isolation and ecological factors. This study enhances our understanding of intraspecific variation within the Sumatran rhinoceros and provides critical insights into the evolutionary morphology of one of the world's most endangered megafauna.

1. Introduction

The extinction of species has seriously threatened the Sumatran rhinoceros, *Dicerorhinos sumatrensis* (Fischer, 1814). In addition to *D. s. lasiotis,* which is believed extinct, there are two extant subspecies of the Sumatran rhinoceros recognized: the Sumatran subspecies (*D. s. sumatrensis*) found in Sumatra and the Bornean subspecies (*D. s. harrissoni*) found in Borneo (Groves, 1965). This species is one of the most endangered mammals in the world, as it is estimated that only a small number of isolated populations remaining in Sumatra (*D. s. sumatrensis*) and Borneo (*D. s. harrissoni*) in recent years (Ahmad Zafir et al., 2011; Goossens et al., 2013; Havmøller et al., 2016). This extant hairy rhinoceros species is considered the smallest species in the Rhinocerotidae family (Groves and Kurt, 1972) and is listed as a critically endangered species according to the International Union for Conservation of Nature (IUCN) Red List (Ellis and Talukdar, 2020). Similar to another extant rhino species native to Indonesia, the Javan rhinoceros (*Rhinoceros sondaicus*), the Sumatran rhinoceros is protected by law. The two subspecies of Sumatran rhinoceros are believed to have descended from population groups of the same species that were separated in the western and eastern parts of Sundaland (Mays et al., 2018). Species extinction in the wild was reported in Malaysian Borneo in 2015 (Havmøller et al., 2016). Previously, the Bornean subspecies was thought to be extinct in the wild in the Indonesian portion of Borneo since the

* Corresponding author.
E-mail addresses: ddcahyadi@apps.ipb.ac.id (D.D. Cahyadi), nhdayat@apps.ipb.ac.id (Nurhidayat).

https://doi.org/10.1016/j.jcz.2026.05.009
Received 13 November 2025; Received in revised form 8 May 2026; Accepted 20 May 2026
Available online 26 May 2026

authority declared their extinction in the 1990s until a small number of individuals were rediscovered in East Kalimantan (Indonesian portion of Borneo; Howard, 2016; Boer, 2020). In March 2016, one of these three individuals, Najaq, was captured and kept in a boma (large captive artificial cage) during the translocation process. Unfortunately, Najaq has not survived in the boma despite the emergency support from the veterinary medical team on site.

The fact that a small population of Sumatran rhinoceros of Borneo was isolated from their relatives that occurred in Sumatra thousands of years ago (Mays et al., 2018), leaves a question about their morphological divergences. The Sumatran rhinoceros subspecies differences were thought to be based on skull and teeth size (Groves, 1967; van Strien, 1974); however, literature is scarce on the anatomical studies of the rhinoceros head skeleton. Studies on the anatomical characteristics of the Sumatran rhinoceros, especially their Bornean subspecies, are still limited. Although geographical variation of the skull has been reported for the Sumatran rhinoceros subspecies by Groves (1967, 1982), detailed anatomical properties of their skull have not been explored yet. This paper describes the morphology of the cranial skeleton of the Sumatran rhinoceros of Borneo (*D. s. harrissoni*), and its anatomical differences compared to the Sumatran subspecies (*D. s. sumatrensis*). Sufficient knowledge of a species' morphology allows scientists to predict the potential use of different traits, even without prior study (Berger, 1994). Therefore, the significance of this study is to provide a better understanding of the morpho-functional characteristics of the Sumatran rhinoceros of Borneo compared to those of the Sumatran subspecies.

2. Materials and methods

2.1. Animal specimens

A female individual of the Bornean subspecies, named Najaq, was found dead on April 5, 2016, during the rescue process in the remote forest in Kutai Barat, East Kalimantan, Indonesia. This individual was buried on-site after the veterinary medical team performed the post-mortem examination. Najaq's skeleton was brought to the Laboratory of Anatomy, School of Veterinary Medicine and Biomedical Sciences, IPB University, Indonesia, after being evacuated from its burial site as per the transport permit for the animal specimen (SATS-DN No. 47/SATS/BKSDA-23/IV/2016) issued by the Natural Resource Conservation Agency of East Kalimantan, Directorate General of Natural Resources and Ecosystem Conservation, Ministry of Forestry and Environment of the Republic of Indonesia. Another skull from an old female Sumatran rhinoceros named Dusun, a specimen from our laboratory collection, was used for comparison. The death of the animals was not related to the present study. Therefore, we did not seek ethical approval for the research since the cranial specimens were obtained from a scientific collection, and no individuals were harmed.

2.2. Head skeleton preparation

Upon arrival at the laboratory, the head of the Bornean rhinoceros were chemically fixed in a 10% formalin solution for two weeks after being soaked in slowly drained water for two days. The skull and mandible were then cleaned by removing any remaining flesh, including rotten muscles, tendons, and ligaments, using a scalpel manually. The bones, devoid of any muscles, were air-dried in an open-air environment. The structure of the cranial and mandibular bones was observed, and the detailed parts were identified according to the nomenclature in Nomina Anatomica Veterinaria (ICVGAN, 2017). The depiction of the rhinoceros skull in Fig. 1A is based on a photograph of a subadult Sumatran rhinoceros head skeleton specimen described in Hagge (2010), highlighting the sutures between the bones for better bone orientation. The bone specimens were captured using a digital camera (Canon® EOS 700D). All observation results were analyzed descriptively and presented as figures.

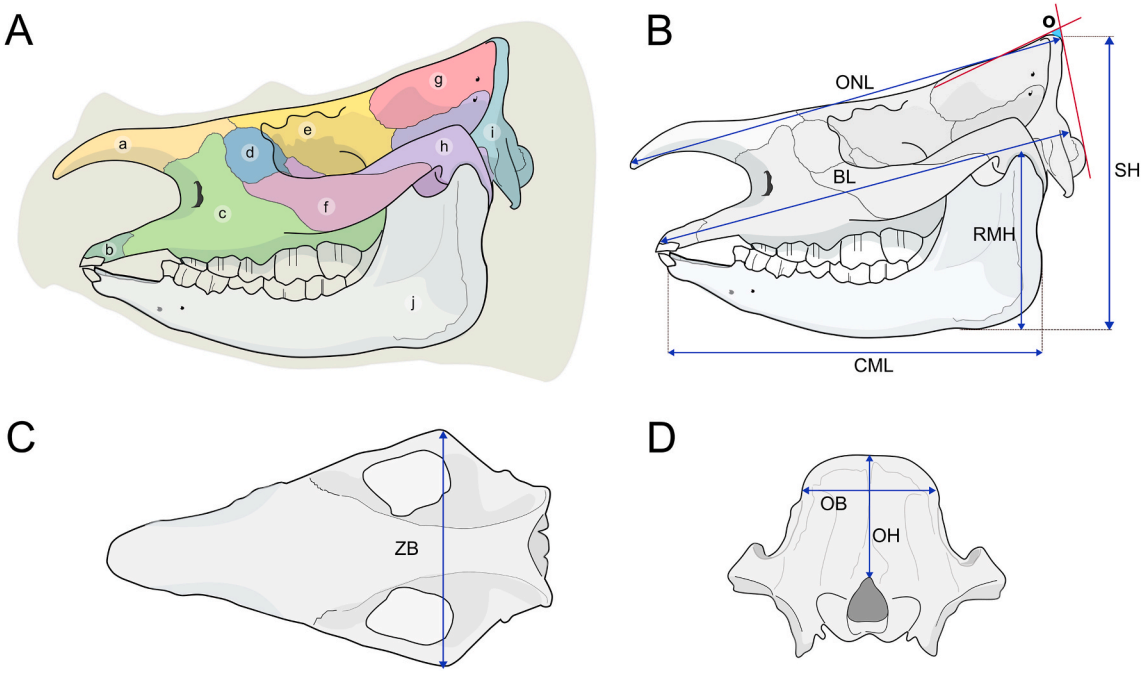

Fig. 1. Schematic illustration of the skull of Sumatran rhinoceros (*Dicerorhinus sumatrensis*). (A) A graphical image depicting the bones constructing the skull of the Sumatran rhinoceros. The image is adapted from the photo of the young Sumatran rhinoceros head skeleton specimens described in Hagge (2010). (a) Nasal bone, *os nasale*; (b) Incisive bone, *os incisivum*; (c) Maxilla, *maxilla*; (d) Lacrimal bone, *os lacrimale*; (e) Frontal bone, *os frontale*; (f) Zygomatic bone, *os zygomaticum*; (g) Parietal bone, *os parietale*; (h) Temporal bone, *os temporale*; (i) Occipital bone, *os occipitale*; (j) Mandible, *mandibula*. (B–D) Morphometric parameters used in the present study. BL, basal length; ONL, occipitonasal length; ZB, zygomatic breadth; CML, corpus of mandible length; RMH, ramus of the mandible height; SH, skull height; OB, occipital breadth; OH, occipital height; o, occipital angle.

2.3. Morphometric data

In addition to morphological observation, the present study included measurements for both subspecies. Skull basal length (BL) was measured from the tip of the nasal bone (*os nasale*) in the rostral to the occipital condyle, while the occipitonasal length (ONL) was measured from the tip of the nasal bone to the dorsal portion of the occipital bone, at the nuchal crest (Fig. 1B). The widest distance between the left and right zygomatic arches (*arcus zygomaticus*) was measured and determined as zygomatic breadth (ZB). The corpus of mandible length (CML) was defined as the distance between the foremost point of the mandible and the *angulus mandibulae*. The greatest height of a ramus of the mandible (RMH), from the topmost point of the *condylus* to *angulus mandibulae*, and the height of the skull (SH) were measured from the lowest part of the ramus of the mandible to the highest portion of the occipital at the nuchal crest. The occipital breadth (OB), which measures the width across the back of the skull at the nuchal crest, and the occipital height (OH), the vertical distance from the dorsal edge of the *foramen magnum* to the highest point of the skull, were also examined. The occipital angle, a metric correlated to the occipital shape (Zeuner, 1934), was also examined. It is defined as the angle between the occipital plane at the back of the skull and the parietal plane at the top of the skull (Zeuner, 1934). The skull morphometry measurement used in the present study is shown in Fig. 1B–D. In addition to the specimens available at our laboratory, we gathered some comparative morphometric data from previous studies (Groves and Kurt, 1972; Guérin, 1980; Groves, 1982; Pandolfi, 2022). We used relevant measurements from those studies whenever they were available. In cases where such measurements were not present, we supplemented the data with measurements based on photographs that included a scale bar. The cranial capacity or volume of the cranial cavity (*cavum cranii*) was estimated using the manual technique. As the cap of bone of the dorsal cranium of the Bornean rhinoceros specimen had been opened for brain sample collection upon her death, the modeling clay was used to fill the cranial cavity. The total clay used to fill the cavity was then put in a graduated cylinder containing a certain amount of water. Based on Archimedes' principle, the weight of the clay is equal to the weight of the displaced water. As the unit weight of water (at room temperature) is 1 kg/m^3, the volume of the displaced water can be calculated. Therefore, the estimated cranial capacity was revealed. However, since the head skeleton of the Dusun specimen has been built to her full body skeleton, we did not measure the cranial capacity from this specimen.

Selected morphometric measurements, BL, ONL, and ZB, between the Bornean and Sumatran subspecies were compared using the Mann–Whitney U Test. A p-value less than 0.05 was considered to indicate a significant difference. Statistical analyses were performed using JASP (Version 0.96.0; JASP Team, 2026), an open-source statistics program supported by the University of Amsterdam, Netherlands.

2.4. The age at death estimation of the najaq

As of now, no specific age estimation technique has been developed for the Sumatran rhinoceros. Studies on dentition-based age estimation in rhinoceros have been reported for the African black rhinoceros *Diceros bicornis* (Goddard, 1970; Hitchins, 1978), white rhinoceros *Ceratotherium simum* (Hillman-Smith et al., 1986), and the extinct woolly rhinoceros *Coelodonta antiquitatis* (Garutt, 1994), by dental eruption and tooth wear pattern assessment. However, since the age estimation based on tooth eruption and wear pattern assessment could be invalid for different types of diets and species, the age at death in the present study was estimated through cementum increment analysis of the maxillary first molar, which was considered a more reliable method across species (Hitchins, 1978; Hillman-Smith et al., 1986; Kirillova et al., 2017). We analyzed the maxillary first molar due to its early eruption and long functional use. The tooth was longitudinally sectioned by using a lapidary saw. The sections were polished using finer abrasives and the image was captured by using digital camera equipped with a macro-lens. Subsequently, the tooth section was examined under a stereomicroscope to identify cementum growth layers and lines of arrested growth (LAGs). No decalcification or staining was conducted, and the dentin-cementum junction was used as a reference point.

According to reports on African rhinoceros, the maxillary first molar usually erupts at around 3 years of age (Goddard, 1970; Hillman-Smith et al., 1986). The first LAG appears in the cementum of the first molar of an African black rhinoceros by the age of 4 years (Hitchins, 1978). Therefore, the number of LAGs/annuli was used as a proxy for age, adding roughly 3 years for a chronological estimate. This method is regarded as approximate and exploratory due to some limitations.

2.5. Computed tomographic imaging

A Computed Tomography (CT) scan was carried out at Azra Hospital, Bogor, West Java, Indonesia. The skull specimen was positioned symmetrically in ventral recumbency on the CT couch. Sequential transverse CT images (0.703125 mm thickness) of the head skeleton (the specimen of Bornean rhinoceros, Najaq) were acquired by CT using a Revolution ACT 32-slice helical scanner (General Electric HealthCare, Beijing, China), which rotated at a speed of 1.00s and emitted radiation of 120 kV and 75 mA. In the present study, we adjusted the CT appearance of the head skeleton structures using window settings with the window width and window level of 2800 and 100 HU, respectively. Sequential CT images generated from the axial, sagittal, and coronal planes in the form of digital imaging and communications in medicine (DICOM) images were saved for bone description and analysis. The image reconstruction program (Bee DICOM Viewer 2.6.1, Sainuo United Medical Technology Co., Ltd., Beijing) was utilized to process the raw data and create various reformatting plans.

3. Results

3.1. Structure of the cranial skeleton

Sumatran rhinoceroses have an elongated skull, elevated on the caudal portion, with a relatively small braincase. The skull measurements for the Bornean subspecies, indicated by the mean and standard deviation (mean ± SD), recorded a basal length (BL) of 450.0 ± 25.6 mm, an occipitonasal length (ONL) of 457.7 ± 18.3 mm, and a width (ZB) of 252.1 ± 11.3 mm (n = 3). In contrast, the Sumatran subspecies showed larger dimensions, with a BL of 496.5 ± 26.0 mm, an ONL of 525.9 ± 24.7 mm, and a ZB of 294.5 ± 19.7 mm (n = 14–15). Both skull length parameters, BL and ONL, were significantly smaller in the Bornean subspecies compared to the Sumatran subspecies, with p-values of 0.027 and 0.009, respectively. Additionally, skull width (ZB) was also significantly smaller in the Bornean subspecies than in the Sumatran subspecies ($p = 0.019$). However, these results should be interpreted cautiously due to the limited sample size and potential influences of individual variation, ontogenetic factors, and sexual dimorphism. Boxplots without whiskers comparing BL, ONL, and ZB between the Bornean and Sumatran subspecies are presented in Fig. 2.

Other morphometric measurements indicated that the Bornean subspecies had a skull height (SH) of 328.9 ± 9.7 mm. The length of the ramus of the mandible (RMH) measured 170.6 ± 21.3 mm, while the length of the corpus of the mandible (CML) was 402.6 ± 36.7 mm. The occipital breadth (OB) and occipital height (OH) were found to be 115.6 ± 4.4 mm and 100.4 ± 17.0 mm, respectively. Conversely, the skull of the Sumatran subspecies was larger overall, with measurements of 350 mm for SH, 183.6 ± 12.1 mm for RMH, 421.3 ± 20.2 mm for CML, 123.2 ± 6.9 mm for OB, and 113.3 ± 11.2 mm for OH. Comparative morphometric data for both subspecies' skulls are provided in Table 1.

In the present study, it was observed that the occipital angle of the Sumatran rhinoceros is acute, with the angle in the Sumatran subspecies

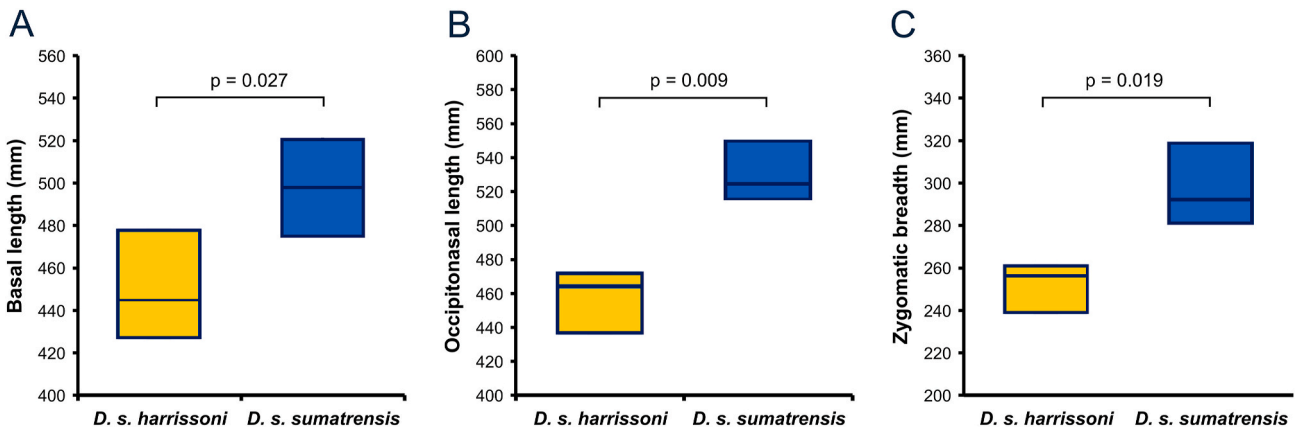

Fig. 2. Multi-panel boxplots (without whiskers) comparing cranial morphometric parameters between Bornean and Sumatran subspecies of the *Dicerorhinus sumatrensis*: (A) basal length, (B) occipitonasal length, and (C) zygomatic breadth. The Bornean subspecies consistently exhibits smaller cranial dimensions. Whiskers are omitted to highlight the central 50% of the data. Significance was determined using the Mann–Whitney U test (n = 3 for *D. s. harrissoni*, n = 14–15 for *D. s. sumatrensis*).

Table 1
Comparative morphometry of the skull of Bornean and Sumatran subspecies of *Dicerorhinus sumatrensis*.

Specimen ID	Measurement (mm)									Occipital angle (°)	Reference
	Sex	BL	ONL	CML	RMH	ZB	SH	OB	OH		
D. s. harrissoni											
Najaq	F	**445**	**437.0**	**376.7**	**155.6**	**256.3**	**322**	**112.5**	**88.4**	**75**	Present study
H.6, 383	-	**427.3**	**464.3**	**428.6**	**185.7**	**239.3**	**335.7**	**-**	**-**	**75**	Groves and Kurt (1972)
D.s.harrissoni (n = 8–10)	-	477.8	471.8	-	-	260.8	-	118.7	112.4	-	Groves (1982)
Mean		450.0	457.7	402.6	170.6	252.1	328.9	115.6	100.4	75.0	
SD		25.6	18.3	36.7	21.3	11.3	9.7	4.4	17.0	0.0	
D. s. sumatrensis											
Dusun	F	**475**	**539**	**407**	**175**	**282**	**350**	**133.3**	**120**	**68**	Present study
Wild females (n = 9)	F	502.1	518.1	-	-	283.6	-	122.9	116.8	-	Groves (1982)
Jenny, NMW 3082	F	498	516.5	-	-	287	-	114	109.5	-	Groves (1982)
Mary, NMW 5026	F	535	550	-	-	297.5	-	123	115	-	Groves (1982)
Bettina, NMB 10259	F	453	473	-	-	278	-	122	103	-	Groves (1982)
Bogor, MZB 8440	F	468	486	-	-	256	-	115	87	-	Groves (1982)
Subur, UZMK 3791	F	457	507	-	-	278	-	118	108	-	Groves (1982)
Wild males (n = 5)	M	520.6	551	-	-	298.8	-	129.6	119.5	-	Groves (1982)
NHMUK 1952-4-1-2	M	**515**	**552**	-	-	-	-	-	-	**70**	Pandolfi (2022)
NHMUK 1948-12-20-1	-	**490.5**	**544**	-	-	-	-	-	-	**69**	Pandolfi (2022)
NHMUK 68-4-15-1	-	**519.0**	**552**	-	-	**320**	-	-	-	**68**	Pandolfi (2022)
NHMUK 1921-2-8-2	M	**524.0**	**544**	-	-	**-**	-	-	-	**70**	Pandolfi (2022)
NHMUK 1921-2-8-3	F	**486.4**	**515.4**	-	-	**-**	-	-	-	**70**	Pandolfi (2022)
NHMUK 1921-2-8-4	F	**481.8**	**515.4**	-	-	**320**	-	-	-	**70**	Pandolfi (2022)
NHMUK 1879-6-14-2	-	-	-	-	-	**320**	-	-	-	-	Pandolfi (2022)
NHMUK 1894-9-24-1	M	-	-	-	-	**300**	-	-	-	-	Pandolfi (2022)
NHMUK 1931-5-28-1	M	-	-	-	-	**318.8**	-	-	-	-	Pandolfi (2022)
D. sumatrensis (n = 17–19)	-	522.8	524.5	435.5	192.1	283.7		130.6	123.1	-	Guérin (1980)
Mean		496.5	525.9	421.3	183.6	294.5		123.2	111.3	69.3	
SD		26.0	24.7	20.2	12.1	19.7		6.9	11.2	1.0	

Note: The numbers written in bold indicate values measured directly in our specimens or based on specimen photographs available in the corresponding articles.

(~70°) slightly sharper than that of the Bornean subspecies (75°). Notably, the Bornean subspecies specimen (Najaq) had an estimated cranial capacity of 610 mL. The Sumatran subspecies specimen (Torgamba), a male who lived to age 30, had a cranial capacity of 897.5 mL.

Observation to the available specimens showed that the dorsal profile of the skull of the Bornean subspecies was slightly concave in the lateral view (Fig. 3A), more than that of the Sumatran subspecies (Fig. 3C). In general, the skull of the Sumatran rhinoceros had rough surfaces on the nasal (*os nasale*), frontal (*os frontale*), zygomatic (*os zygomaticum*), temporal (*os temporale*), and occipital (*os occipitale*) bones. In the rostral part, the dorsal surface of the nasal bone was rough and relatively wide, both in the Bornean and Sumatran rhinoceros specimens. From the lateral view, the specimen of the Bornean subspecies had a relatively straight tip of the nasal bone, whereas it was ventrally curved in the Sumatran subspecies specimen (Fig. 3C). The frontal bone, which constructs the dorsal part of the skull and the roof of the nasal cavity (*cavum nasi*), was rough on its dorsal surface in both subspecies (Fig. 4A–C). In both subspecies, a relatively short facial crest (*crista facialis*) was observed crossing the zygomatic bone and extending to the posterior part of the maxilla (*maxilla*), a bone that constructs the facial part of the skull in the lateral part (Fig. 3A–C). The thickened alveolar ridge in its ventrolateral part, containing the alveoli for the premolars and molars, was also observed. Additionally, a well-developed infraorbital foramen (*foramen infraorbitale*) was also observed in the anterodorsal of this bone, above the second premolar.

The parietal bone (*os parietale*) was situated caudal to the frontal bone and constructed the roof of the cranial cavity (*cavum cranii*) of the Sumatran rhinoceros. The parietal surface of the Bornean rhinoceros

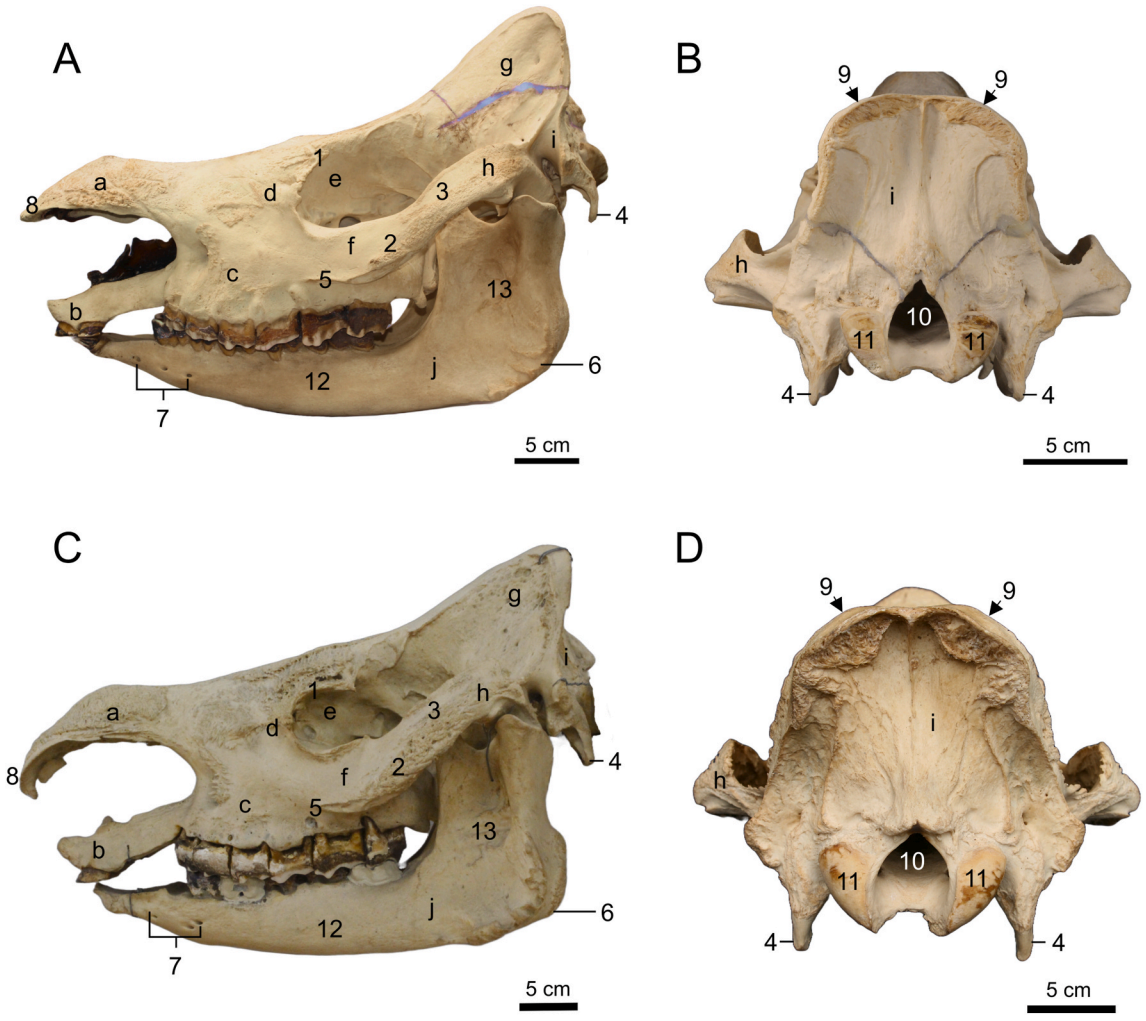

Fig. 3. The skull of the Bornean (A and B) and Sumatran subspecies (C and D) of Sumatran rhinoceros, lateral and caudal view.
(a) Nasal bone, *os nasale*; (b) Incisive bone, *os incisivum*; (c) Maxilla, *maxilla*; (d) Lacrimal bone, *os lacrimale*; (e) Frontal bone, *os frontale*; (f) Zygomatic bone, *os zygomaticum*; (g) Parietal bone, *os parietale*; (h) Temporal bone, *os temporale*; (i) Occipital bone, *os occipitale*; (j) Mandible, *mandibula*; 1. *Crista frontalis externa*; 2. *Processus temporalis os zygomaicum*; 3. *Processus zygomaticus os temporale*; 4. *Processus jugularis*; 5. *Crista facialis*; 6. *Angulus mandibulae*; 7. *Foramen mentale*; 8. *Apex nasi;* 9. *Crista nuchae*; 10. *Foramen magnum*; 11. *Condylus mandibulae*; 12. *Corpus mandibulae;* 13. *Ramus mandibulae*. Scale bar = 5 cm.

specimen was convex, as seen in the skull of the Sumatran subspecies, but relatively narrower (Fig. 4A–C). The zygomatic arch was observed to rise sharply (the temporal process of the zygomatic bone, *processus temporalis os zygomaticum*) above the tooth row at the level of the second molar, caudal to the maxillary bone (Fig. 4A–D). This structure was arched dorsally, attaining the level of the dorsal orbital border at the temporal part (zygomatic process of the temporal bone, *processus zygomaticus os temporale*). Rhinoceroses have an open orbit due to the absence of the zygomatic process of the frontal bone at the superior margin of the orbit (Fig. 3A–C). The caudal surface of the skull was constructed by the occipital bone. The nuchal crest (*crista nuchae*) was located in the dorsal portion of the occipital bone, at the highest part of the skull. The Bornean subspecies displayed a more obtuse occipital angle compared to the Sumatran subspecies, which had a sharper occipital angle. Additionally, it was noted that the skull of the Bornean subspecies differs from that of the Sumatran subspecies in two main ways: it features a narrower rough surface at the ventral portion of the nuchal crest and a laterally narrower occipital surface area when viewed from the rear (see Fig. 3B–D). These differences are further illustrated by the values of OB and OH presented in Table 1.

In both subspecies of Sumatran rhinoceros, two branches of the mandible (*corpus mandibula*) form a “V" shaped intermandibular space in the dorsal view (Fig. 5A and B). The diastema (*margo interalveolaris*), a space between the premolar and lower incisor alveoli, was large. In the present study, three mental foramina (*foramina mentalia*) were observed in the mandible of the Bornean subspecies, the same number observed in the Sumatran subspecies (Fig. 5C and D). However, these three foramina in the Bornean subspecies were aligned horizontally at the level of the third, second, and rostral to the second premolars from the caudal to the rostral position. In contrast, we observed variations in the positions of these foramina on the left and right sides of the Sumatran subspecies specimen.

3.2. Dental formula, tooth wear, and the age-at-death determination

It is widely known that the dental formula of the Sumatran rhinoceroses is I1/1 C0/0 P3/3 M3/3. However, it was observed that the Najaq specimen displayed the dental formula as I2/1 C0/0 P3/3 M3/3, with 30 permanent teeth in total. In this "Najaq" specimen, the first and second incisors were observed in the upper jaw, with the latter relatively smaller (Fig. 3A and 4B). These incisors were chisel-shaped and pointed in the cranioventral direction. In contrast, the second incisor was not observed on the specimen of the Sumatran subspecies, Dusun, whose dental formula was I1/1 C0/0 P3/3 M3/3. It is important to note for the Dusun specimen that a pair of lower incisors was extracted during her lifetime and, therefore, are not present in the specimen (Fig. 5B–D).

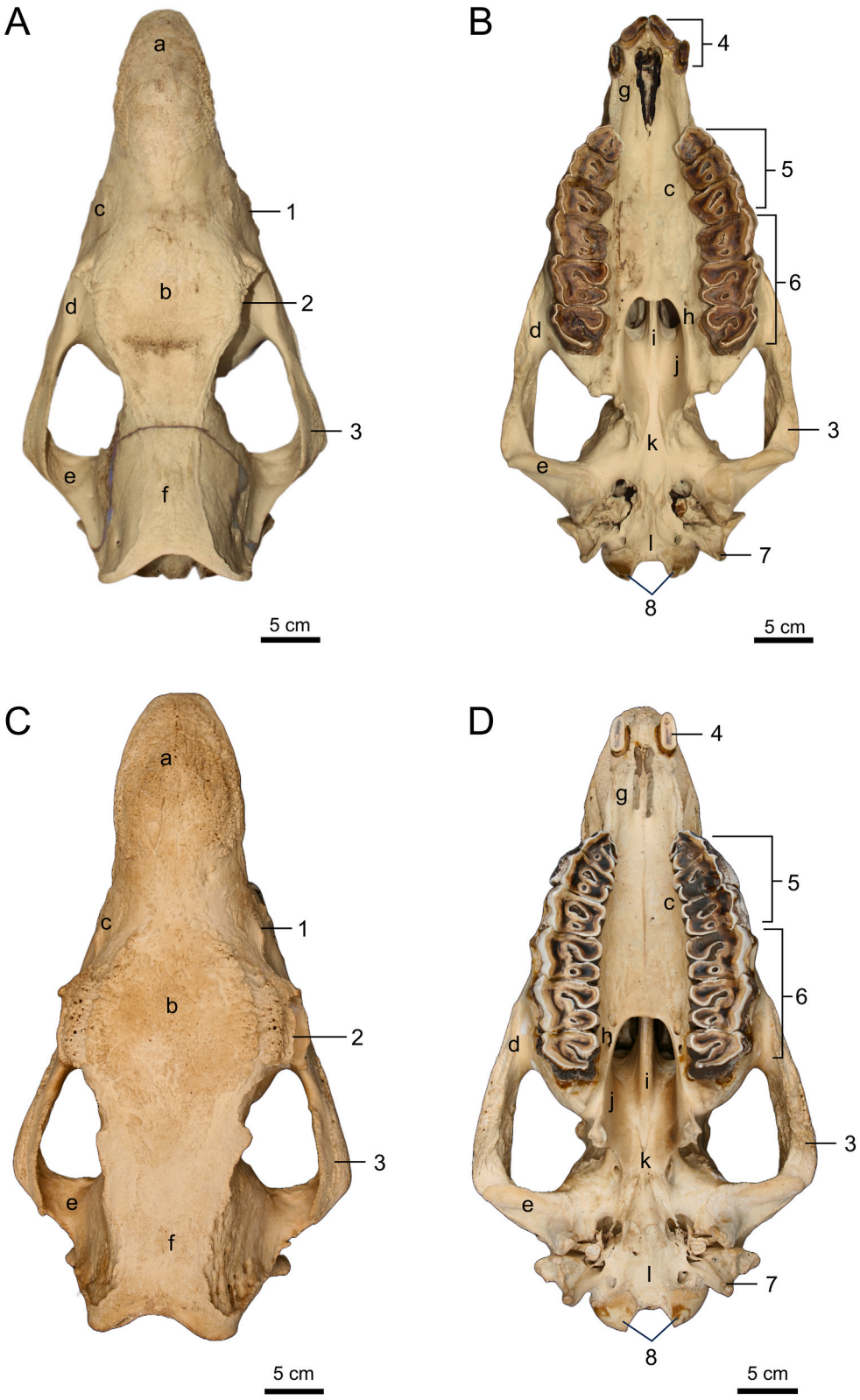

Fig. 4. The skull of the Bornean (A and B) and Sumatran subspecies (C and D) of Sumatran rhinoceros, dorsal and ventral view.
(a) Nasal bone, *os nasale*; (b) Frontal bone, *os frontale*; (c) Maxilla, *maxilla*; (d) Zygomatic bone, *os zygomaticum*; (e) Temporal bone, *os temporale*; (f) Parietal bone, *os parietale*; (g) Incisive bone, *os incisivum*; (h) Palatine bone, *os palatinum*; (i) Vomer, *vomer*; (j). Pterygoid bone, *os pterygoideum*; (k) Sphenoid bone, *os sphenoidale*; (l) Occipital bone, *os occipitale*; 1. *Crista facialis*; 2. *Crista frontalis*; 3. *Arcus zygomaticus*; 4. *Dentes incisivi*; 5. *Dentes premolares*; 6. *Dentes molares*, 7. *Processus jugularis*; 8. *Condylus occipitalis*. Scale bar = 5 cm.

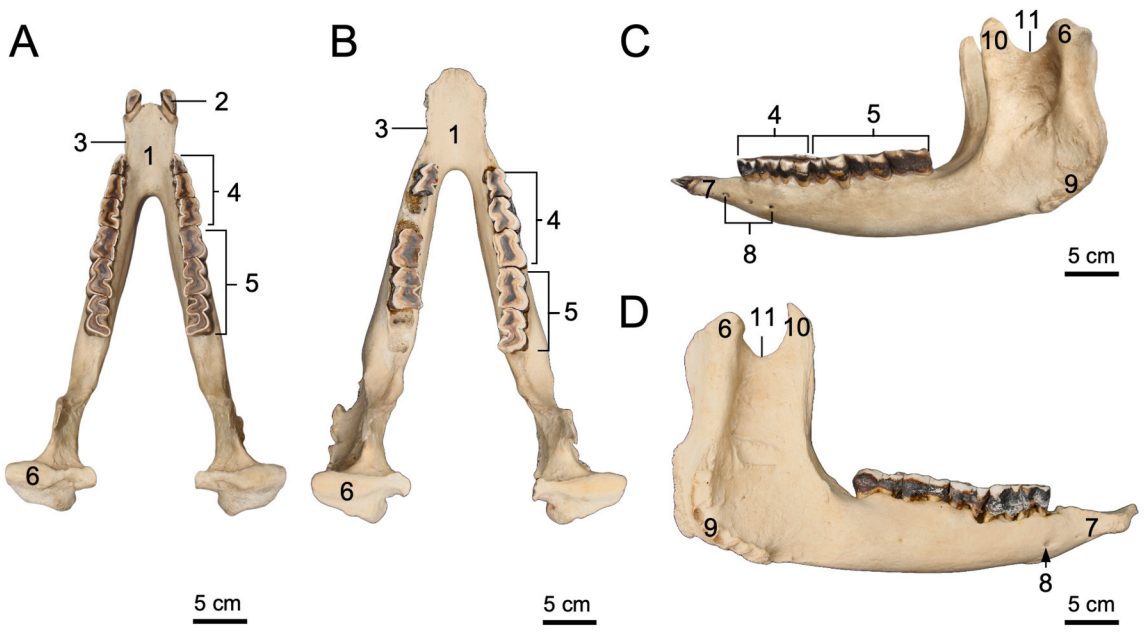

Fig. 5. Mandible of the Bornean (A and C) and Sumatran subspecies (B and D) of Sumatran rhinoceros, in dorsal and lateral view, respectively. 1. *Facies lingualis*; 2. *Dentes incisivi*; 3. *Margo interalveolaris* (diastema); 4. *Dentes premolares*; 5. *Dentes molares*; 6. *Condylus mandibularis*; 7. *Facies labialis*; 8. *Foramen mentale*; 9. *Angulus mandibulae*; 10. *Processus coronoideus*; 11. *Incisura mandibulae*. Scale bar = 5 cm.

Moreover, its second lower premolars were completely worn down in this individual, and their alveoli were overgrown at the time of death, so that the first lower premolars could not be observed in the specimen (Fig. 3C and 4D). The maxillary premolars and molars of both subspecies showed a wider surface than those of the mandibular premolars and molars. Thus, the buccal side of maxillary premolar and molar crowns is taller than the lingual side. In the Bornean rhinoceros specimen, a pair of small tusk-like incisors was observed in the lower jaw pointed craniodorsally (Fig. 5A–C). However, a missing or incomplete specimen, as mentioned earlier, prevented observation of the second incisors in the Dusun specimen (Fig. 5B–D).

In general, the tooth wear in premolars and molars of the lower jaw was greater than that of the upper jaw, with the premolars exhibiting greater tooth wear than the molars. The structural appearance of the prefossette, crochet, postfossette, and medivallum was used to evaluate the tooth wear of the maxillary premolars and molars as previously described in Hitchins (1978). The tooth wear of maxillary premolars and molars is summarized in Table 2. Briefly, our findings showed that the "Najaq" specimen exhibits excessive tooth wear, characterized by the isolated prefossette, crochet, and postfossette structures of the premolars. Observation of the section of the maxillary first molar showed a thick accumulation of cementum within the cementum pad (Fig. 6). However, the incremental structures appeared closely spaced, overlapping, and poorly differentiated. This pattern is consistent with the progressive narrowing of cementum increments with increasing age, which complicates accurate layer discrimination. Due to the limited clarity of individual LAGs/annuli, it was not possible to reliably determine the exact number of cementum growth layers, even under magnification. Nevertheless, the observed density and pattern of incremental structures suggest the presence of more than 20 growth layers, indicating that the "Najaq" specimen was an old adult at the time of death.

Table 2
Tooth wear patterns observed in the maxillary teeth of the Najaq specimen used in this study.

Dental	Prefossette	Postfossette	Crochet	Medivallum
Premolares II	Isolated	Isolated	Absent	Absent
Premolares III	Isolated	Isolated	Absent	Absent
Premolares IV	Isolated	Isolated	Absent	Absent
Molares I	Isolated	Isolated	Absent	Absent
Molares II	Present	Isolated	Present (almost disappear)	Present
Molares III	Present	Absent	Present	Present

3.3. Computed tomography images

Images of the three-dimensional reconstruction of the Bornean rhinoceros skull (Najaq specimen) in the lateral view are shown in Fig. 7A. Sequential transverse CT images from the rostral to the caudal portion of the head skeleton, corresponding to segments 1–7 described in Fig. 7B, are presented in Fig. 7C. These CT images in the transversal plane confirmed that maxillary premolars and molars had a wider surface than those of the mandibular teeth; therefore, the wear on the lingual side of the teeth was more significant (Fig. 7C, segments 2–3). The nasal sinus structure in the nasal bone is shown in the transversal plane of the CT image (Fig. 7C, segments 1–4), describing the different sizes in the different areas. A quite large maxillary sinus structure was observed in the CT image, as shown in Fig. 7C, segments 3 and 4. In particular, the frontal sinuses are relatively small, while the parietal sinuses are larger as the skull's external shape is caudally inclined at the level of the parietal and occipital bones (Fig. 7B and C, segments 5–7). Generally, thin bony intersinus septa were present in those sinus structures.

4. Discussions

Although the skull profile of the Bornean subspecies in the lateral view was considerably concave, it was not as pronounced as that of our Javan rhinoceros specimen or previously described specimens (Cave, 1985; Groves and Leslie, 2011). A rough dorsal surface of the nasal and frontal bones is associated with the attachment base of the nasal and frontal horns, respectively (Hieronymus et al., 2006). In the Bornean subspecies, a narrower parietal surface of the parietal bone, as seen in the "Najaq" specimen, is thought to be associated with the smaller cranial cavity relative to the Sumatran subspecies. The smaller cranial capacity of the Bornean subspecies was suggested to be following their

Fig. 6. The vertical section of the maxillary first molar (M1) in the rostrocaudal direction displays growth layers in the dental cementum LAGs highlighted with white arrows, indicating the age of Najaq at the time of her death.

smaller body size compared to that of the Sumatran subspecies (van Strien, 1974), and was thought to be the smallest among the extant rhinoceros in the world at the comparable age (Rookmaaker, 1984). Groves (1965) earlier described that the specimens of Bornean rhinoceros (*Didermocerus sumatrensis harrissoni,* later it was classified as *Dicerorhinus sumatrensis harrissoni*) were markedly smaller than the other populations. Comparative morphometric data presented in this study suggest that the skull size of the Bornean subspecies is significantly smaller than that of the Sumatran subspecies. However, this finding requires further confirmation with a larger sample size, with consideration of the potential effects of individual, ontogenetic, and sexual variation. Moreover, since image-based measurements are incorporated in the present study, despite being calibrated using their scale bars, certain factors such as perspective distortion may affect the measurements; therefore, these data were used only as supplementary information and interpreted with caution.

The parietal bones of the rhinoceros contribute to constructing the roof of the braincase, similar to that of Tapiridae (Holbrook, 2002; Moyano and Giannini, 2017) and horses (Morrow et al., 2000; Goodarzi et al., 2021). The zygomatic arch in rhinoceroses is formed by the maxilla, zygomatic, and temporal bones, without contribution from the frontal bone, similar to that of the Tapiridae (Moyano and Giannini, 2017; Dumbá et al., 2019), which are phylogenetically close to Rhinocerotidae. Based on our previous postmortem observations in Sumatran rhinoceros, we suggest that a well-developed zygomatic arch is associated with strong masticatory muscles (*m. masseter*, both deep and superficial layers) attached to it, while only small parts originate from the facial crest of the maxilla. This characteristic has also been noted in several studies on both extinct and extant rhinoceroses, although muscle development varies among different rhinocerotid species (Beddard and Treves, 1889; Borsuk-Białynicka, 1973; Ansón and Hernández Fernández, 2013; Wang et al., 2017).

The Bornean subspecies has a more obtuse occipital angle, which may slightly affect the atlanto-occipital articulation compared to the Sumatran subspecies. Zeuner (1934) was the first study to quantitatively examine the occipital shape, particularly the occipital angle. The study found that occipital shape correlates with head posture and feeding behavior, noting that browsing rhinoceroses have a relatively more obtuse occipital angle (between the occipital and parietal planes) than grazing species. However, in the present study, this descriptive anatomical comparison between two subspecies of Sumatran rhinoceros should be viewed cautiously, as it does not imply functional differences in cervical mobility, which is generally low in Rhinocerotidae (Belyaev et al., 2023). Moreover, the narrower nuchal crest surface and occipital surface area (in the posterior view) in the Bornean subspecies are suggested to be correlated with the smaller nuchal ligament and cervical muscles in general compared to those of the Sumatran subspecies. The nuchal crest, in addition to the external occipital protuberance, serves as the attachment site of the nuchal ligaments (Gellman et al., 2002), which support the relatively big head of this animal.

Variation in the number and position of mental foramina observed in the mandible likely reflects differences in the branching pattern of the mental nerve, as reported in previous studies of the Sumatran rhinoceros and other rhinoceros species (Groves and Kurt, 1972; Cave, 1985; Bordoloi et al., 1995; Hagge, 2010; Groves and Leslie, 2011).

The anterior dentition of rhinoceroses has historically been subject to differing interpretations, particularly regarding the homology of tusk-like teeth. Earlier studies variably described these structures as canines or incisors (Groves and Kurt, 1972; van Strien, 1974; Banks, 1978; Bordoloi et al., 1995; Cerdeño, 1995). However, after a comprehensive analysis by Radinsky (1966), based on paleontological data, the Rhinocerotidae family is known to be characterized by having chisel-shaped upper incisors (I1) and tusk-like lower incisors (I2). This interpretation is now widely accepted in both extant and fossil rhinoceroses' literature (Groves and Leslie, 2011; Groves, 2017; Avedik et al., 2023; Lu et al., 2023). Moreover, the first lower incisor (I1) is absent in *Dicerorhinus* and two African species (Tougard et al., 2001), but common in *Rhinoceros* (Cerdeño, 1995). In the African rhinoceros, the lower incisors are only present in the deciduous teeth but are absent in the permanent teeth (Groves, 1972; Hitchins, 1978; Hillman-Smith and Groves, 1994).

Although many studies have described that the Sumatran rhinoceros possesses a pair of upper incisors (I1), second upper incisors (I2) can occasionally occur, including the observed second upper incisor (I2) of the "Najaq" specimen in the present study. A male Sumatran rhinoceros specimen at the Sumatran Rhino Sanctuary in Way Kambas, Lampung, was previously reported to have dental alveoli believed to be for the upper canine teeth. However, upon closer observation, it was determined that these alveoli might actually be for small second upper incisors. Such small alveoli were also recorded in the adult female Sumatran rhino from Mogok, Myanmar (Pocock, 1944). The presence of two pairs of upper incisors in the examined specimen is likely an individual variation or developmental anomaly rather than a diagnostic trait of *D. s. harrissoni*, particularly given that previous studies of multiple specimens have consistently reported a single pair of upper incisors (Groves and Kurt, 1972).

It is known that herbivores have well-developed premolars and molars for grinding plants, but the incisors observed in the Sumatran rhinoceros may contribute to the mechanical properties of cutting the branches of vegetation, in addition to the utilization of their prehensile lips. This is in accordance with the basic incisor shearing mechanism

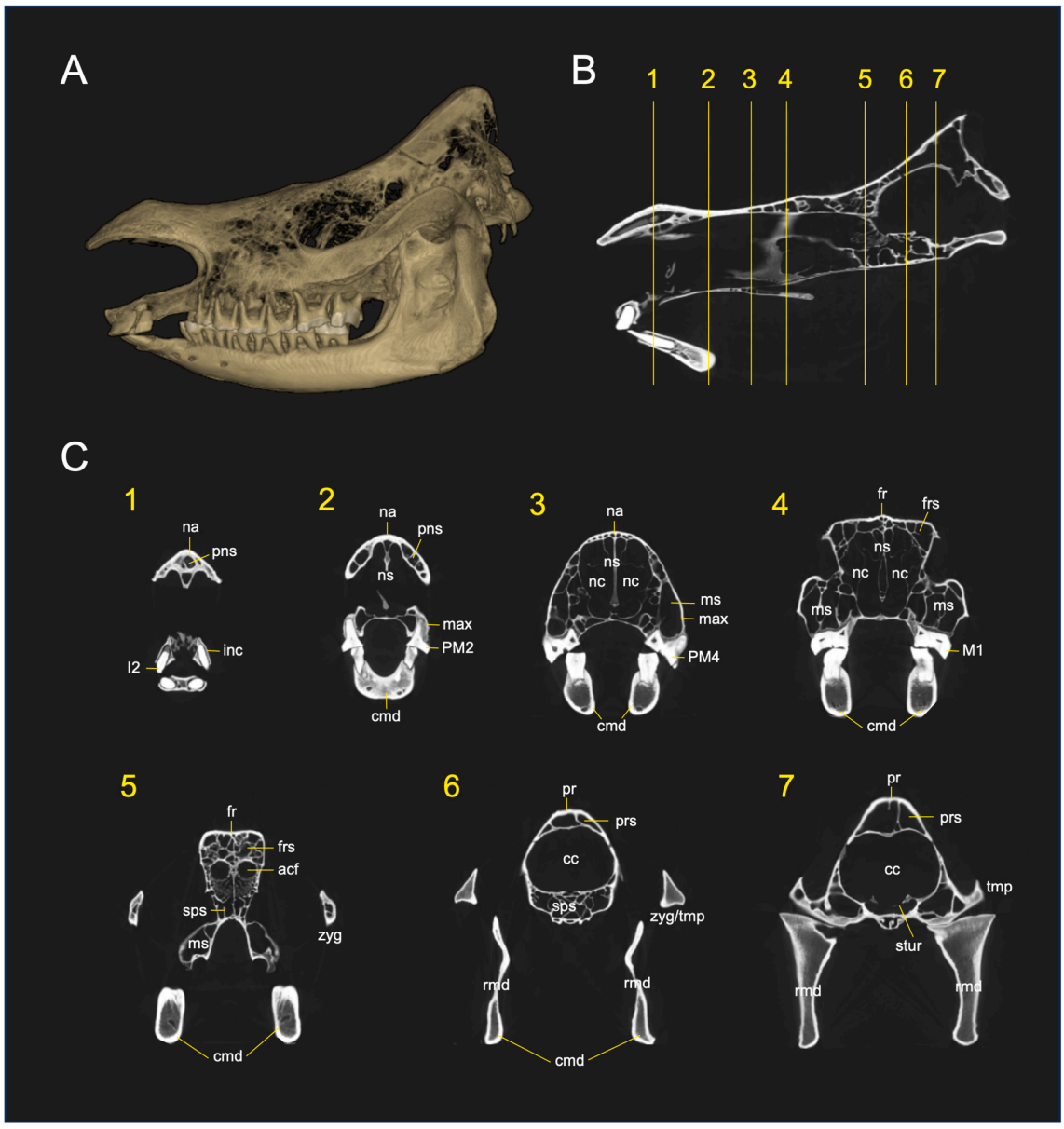

Fig. 7. Computed tomography (CT) imaging of Najaq's skull. (A) Three-dimensional reconstruction image in the lateral view, (B) Mid-sagittal CT image of the Najaq's skull that represents the level of the slices of this study. (C) Transverse CT images correspond to segments 1–7 in (B), respectively. na: nasal bone; pns: paranasal sinuses; inc: incisive bone; ns: nasal septa; nc: nasal cavity; max: maxilla; ms: maxillary sinuses; cmd: body of mandible; fr: frontal bone; frs: frontal sinuses; acf: anterior cranial fossa; sps: sphenoidal sinuses; zyg: zygomatic bone (temporal process of the zygomatic arch); pr: parietal bone; prs: parietal sinuses; cc: cranial cavity; tmp: temporal bone (zygomatic process of the zygomatic arch); rmd: ramus of mandible; stur: sella turcica; I2: second incisors; PM2: second premolar; PM4: fourth premolar; M1: first molar.

discussed by Radinsky (1966), in which Rhinocerotid incisors are functionally specialized into a shearing system involving the upper I1 and lower I2, indicating a primary role in cutting vegetation prior to mastication. However, the variation in the incisor number should not be interpreted as a morphofunctional adaptation, particularly in the feeding behavior.

Although grazing species are generally associated with greater molar wear due to more abrasive diets compared to browsing species (Solounias et al., 1994), such distinctions may become less evident in older individuals due to cumulative wear. The Najaq specimen's maxillary tooth wear, as described in the Results section, displays a similar pattern to the tooth wear of the old adult individuals of the African black and white rhinoceros. The dental wear corresponds to the age class XVI (30–33 years) described by Hitchins (1978) and age class XIII (20–28 years) described by Hillman-Smith et al. (1986), respectively.

In animals, cementochronology appears to be one of the commonly used method in determining the age at death (Reimers and Nordby, 1968; Amano et al., 2004; Oi, 2009; Vipin et al., 2018; Adams and Blanchong, 2020). Numerous known mammal species have growth lines called cementum annuli that periodically form on their dental cementum (Klevezal, 1995), which are possibly utilized for age estimation (Grue and Jensen, 1979). The determination of the age at death by calculating the cementum lines could be done in the maxillary first molar, as it is recognized as the first erupted, before other molars and the permanent premolar teeth (Kirillova et al., 2017). Since we were unable to count the number of LAGs/annuli in the Najaq specimen reliably, it was not possible to determine the exact number of cementum growth layers. Given these limitations, the age estimate derived from cementum analysis should be regarded as approximate, and the results primarily support classifying the specimen as an old adult individual rather than

providing a precise chronological age.

The transversal ridge structures in the horn were also described as a morphological feature that can be used for age estimation of the woolly rhinoceros, *C. antiquitatis* (Fortelius, 1983; Garutt, 1998; Chernova and Kirillova, 2010; Kirillova and Shidlovskiy, 2010; Boeskorov et al., 2025). A periodic banding pattern observed in the rhinoceros' horns is also a recording structure in modern rhinoceroses (Hieronymus et al., 2006), but the study of modern rhinoceros horns requires either tissue sectioning or CT scanning. However, this method has not yet been refined, and its limitations are unknown for either the Sumatran rhinoceros or other modern rhinoceroses.

Computed tomographic imaging of the Najaq specimen provides a better insight into the cranial structure of the Sumatran rhinoceros, in particular, the Bornean subspecies. We suggest that the relative size of the nasoconchal sinus (nasal sinus and dorsal conchae sinus) in the Bornean rhinoceros is not as large as that reported in the African white rhinoceros (Gerard et al., 2018). The frontal sinuses in the Rhinocerotidae are proportionally smaller than those reported in some species of Tapiridae (Colbert, 2003). The function of all those air-filled cavity structures in the Sumatran rhinoceros is unclear. The nasal and dorsal conchae sinuses in the rhinoceros' skull, in particular, are believed to help in absorbing the force transmitted from the horn (Gerard et al., 2018). The sinuses help maintain the external shape of the head skeleton while minimizing its weight, as discussed in many studies (Preuschoft et al., 2002). Nevertheless, the rhinoceros skull remains relatively massive and is associated with a relatively sharp occipital angle and a broad occipital surface, which together provide an extensive area for the attachment of bulky and strong head extensor musculature. The current common hypothesis suggests that the sinuses are a non-functional structures developed as a consequence of so-called 'opportunistic pneumatization' due to the mechanical demands put on the skull (Farke, 2010).

5. Conclusions

Our study has shown the morphological divergences in the skull of the Bornean and Sumatran subspecies of the Sumatran rhinoceros. Overall, morphometric measurements on the Sumatran rhinoceros skulls highlight that the skull size of the Bornean subspecies is significantly smaller than that of the Sumatran subspecies, as indicated by the basal length, occipitonasal length, and zygomatic breadth. Moreover, the Bornean rhinoceroses possess a more obtuse occipital angle compared to that of their relative. The variations observed could be attributed to the relationship between the size of other body parts (allometry), the adaptation of animals to their environment, or the interdependence of various morphological features (morphological integration). The sample used in this study was limited, in particular, the Bornean subspecies of the Sumatran rhinoceros; thus, our results must be interpreted carefully. Increasing the sample size and specimen diversity in the future will aid in a better understanding of possible morphological evolution in the Sumatran rhino subspecies. Additionally, dental eruption and tooth wear in Sumatran rhinoceroses need to be recorded from the living populations and comprehensively analyzed in future studies to support the establishment of the dentition-based age estimation for Sumatran rhinoceros.

Funding

This research received no specific grant from funding agencies in the public, commercial, or not-for-profit sectors.

CRediT authorship contribution statement

Danang Dwi Cahyadi: Conceptualization, Formal analysis, Investigation, Methodology, Visualization, Writing – original draft, Writing – review & editing. **Deanty Chairunnisa:** Formal analysis, Investigation, Visualization, Writing – original draft, Writing – review & editing. **Supratikno:** Investigation, Validation, Writing – review & editing. **Savitri Novelina:** Investigation, Writing – review & editing. **Chairun Nisa':** Investigation, Writing – review & editing. **Srihadi Agungpriyono:** Investigation, Writing – review & editing. **Dedi Chandra:** Investigation, Writing – review & editing. **Kurnia Oktavia Khairani:** Investigation, Writing – review & editing. **Zulfiqri:** Investigation, Writing – review & editing. **Muhammad Agil:** Investigation, Writing – review & editing. **Jono Adiputro:** Resources, Writing – review & editing. **Matheas Ari Wibawanto:** Resources, Writing – review & editing. **Nurhidayat:** Conceptualization, Formal analysis, Methodology, Resources, Supervision, Validation, Writing – review & editing.

Declaration of competing interest

The authors declare that they have no known competing financial interests or personal relationships that could have appeared to influence the work reported in this paper.

Acknowledgments

The authors thank the Ministry of Forestry of the Republic of Indonesia and the Natural Resources Conservation Agency of East Kalimantan for the technical support in the provision of skeleton specimens of the Najaq, including their assistance during the evacuation from the remote forest in Kutai Barat, East Kalimantan, to the Laboratory of Anatomy at IPB University, Bogor, West Java. We thank Holid and Mad Dia for their technical support in processing the Najaq specimen.

Data availability

Data will be made available on request.

References

Adams, D.M., Blanchong, J.A., 2020. Precision of cementum annuli method for aging male white-tailed deer. PLoS One 15 (5), e0233421. https://doi.org/10.1371/journal.pone.0233421.

Ahmad Zafir, A.W., Payne, J., Mohamed, A., Lau, C.F., Sharma, D.S.K., Alfred, R., Williams, A.C., Nathan, S., Ramono, W.S., Clements, G.R., 2011. Now or never: what will it take to save the Sumatran rhinoceros *Dicerorhinus sumatrensis* from extinction? Oryx 45 (2), 225–233. https://doi.org/10.1017/S0030605310000864.

Amano, M., Oi, T., Hayano, A., 2004. Morphological differentiation between adjacent populations of Asiatic black bears, *Ursus thibetanus japonicus*, in northern Japan. J. Mammal. 85 (2), 311–315. https://doi.org/10.1644/1545-1542(2004)085<0311:MDBAPO>2.0.CO;2.

Ansón, M., Hernández Fernández, M., 2013. Artistic reconstruction of the appearance of *Prosantorhinus* Heissig, 1974, the teleoceratine rhinoceros from the middle Miocene of somosaguas. Span. J. Palaeont. 28 (1), 43–53.

Avedik, A., Duque-Correa, M.J., Clauss, M., 2023. Avoiding the lockdown: morphological facilitation of transversal chewing movements in mammals. J. Morphol. 284 (2), e21554. https://doi.org/10.1002/jmor.21554.

Banks, E., 1978. Mammals from Borneo. Brunei Mus. J. 4 (2), 165–227.

Beddard, F.E., Treves, F., 1889. On the anatomy of *Rhinoceros sumatrensis*. Proc. Zool. Soc. Lond. 57 (1), 7–25. https://doi.org/10.1111/j.1469-7998.1889.tb06740.x.

Belyaev, R.I., Kuznetsov, A.N., Prilepskaya, N.E., 2023. Truly dorsostable runners: vertebral mobility in rhinoceroses, tapirs, and horses. J. Anat. 242, 568–591. https://doi.org/10.1111/joa.13799.

Berger, J., 1994. Science, conservation, and black rhinos. J. Mammal. 75 (2), 298–308. https://doi.org/10.2307/1382548.

Boer, C., 2020. Is rhino population in Kalimantan on the edge of extinction? Adv. Ecol. Environ. Res. 5 (10), 271–275.

Boeskorov, G.G., Cheprasov, M.Y., Novgorodov, G.P., Shchelchkova, M.V., Prilepskaya, N.E., Belyaev, R.I., 2025. The longest known rhino horn from the permafrost of Yakutia offers insights into woolly rhinoceros morphology, palaeoecology and sexual dimorphism. J. Zool. 327 (4), 337–348. https://doi.org/10.1111/jzo.70064.

Bordoloi, C.C., Borthakur, S., Talukdar, S.R., Kalita, S.N., Baishya, G., Kalita, H., 1995. Mandible of the great Indian one horned rhinoceros (*Rhinoceros unicornis*). Indian Vet. J. 72, 838–842.

Borsuk-Białynicka, M., 1973. Studies on the Pleistocene rhinoceros *Coelodonta antiquitatis* (blumenbach). Palaeontol. Pol. 29, 5–94.

Cave, A.J.E., 1985. An unrecorded specimen of the Javan rhinoceros (*Rhinoceros sondaicus*). J. Zool. 207 (4), 527–535. https://doi.org/10.1111/j.1469-7998.1985.tb04949.x.
Cerdeño, E., 1995. Cladistic analysis of the family Rhinocerotidae (Perissodactyla). Am. Mus. Novit. 3143, 1–25.
Chernova, O.F., Kirillova, I.V., 2010. New data on horn morphology of the woolly rhinoceros (*Coelodonta antiquitatis* Blumenbach, 1799). Proc. Zool. Inst. RAS 314 (3), 333–342. https://doi.org/10.31610/trudyzin/2010.314.3.333.
Colbert, M., 2003. *Tapirus indicus*, Asian tapir. Digital morphology. http://digimorph.org/specimens/Tapirus_indicus/. (Accessed 8 March 2024).
Dumbá, L.C.C.S., Parisi Dutra, R., Cozzuol, M.A., 2019. Cranial geometric morphometric analysis of the genus *Tapirus* (Mammalia, Perissodactyla). J. Mammal. Evol. 26, 545–555. https://doi.org/10.1007/s10914-018-9432-2.
Ellis, S., Talukdar, B., 2020. *Dicerorhinus sumatrensis*. The IUCN red list of threatened species 2020: E.T6553A18493355. https://dx.doi.org/10.2305/IUCN.UK.2020-2.RLTS.T6553A18493355.en. (Accessed 15 November 2024).
Farke, A.A., 2010. Evolution and functional morphology of the frontal sinuses in Bovidae (Mammalia: Artiodactyla), and implications for the evolution of cranial pneumaticity. Zool. J. Linn. Soc. 159 (4), 988–1014. https://doi.org/10.1111/j.1096-3642.2009.00586.x.
Fortelius, M., 1983. The morphology and paleobiological significance of the horns of *Coelodonta antiquitatis* (Mammalia: Rhinocerotidae). J. Vertebr. Paleontol. 3 (2), 125–135. https://doi.org/10.1080/02724634.1983.10011964.
Garutt, N.V., 1994. Dental ontogeny of the woolly rhinoceros *Coelodonta antiquitatis* (Blumenbach, 1799). CRANIUM 11 (1), 37–48.
Garutt, N., 1998. Neue Angaben über die Hörner des Fellnashorns *Coelodonta antiquatis*. Deinsea 4 (1), 25–40.
Gellman, K.S., Bertram, J.E.A., Hermanson, J.W., 2002. Morphology, histochemistry, and function of epaxial cervical musculature in the horse (*Equus caballus*). J. Morphol. 251 (2), 182–194. https://doi.org/10.1002/jmor.1082.
Gerard, M.P., Glyphis, Z.G., Crawford, C., Blikslager, A.T., Marais, J., 2018. Identification of a nasoconchal paranasal sinus in the white rhinoceros (*Ceratotherium simum*). J. Zoo Wildl. Med. 49 (2), 444–449. https://doi.org/10.1638/2017-0185.1.
Goddard, J., 1970. Age criteria and vital statistics of a black rhinoceros population. African J. Ecol. 8 (1), 105–121. https://doi.org/10.1111/j.1365-2028.1970.tb00834.x.
Goodarzi, N., Zehtabvar, O., Tohidifar, M., 2021. Applied anatomy of the skull in the Arabian horse: a computed tomographic, cross-sectional, volumetric and morphometric study. Vet. Med. Sci. 7, 2225–2233. https://doi.org/10.1002/vms3.618.
Goossens, B., Salgado-Lynn, M., Rovie-Ryan, J.J., Ahmad, A.H., Payne, J., Zainuddin, Z. Z., Nathan, S.K.S.S., Ambu, L.N., 2013. Genetics and the last stand of the Sumatran rhinoceros *Dicerorhinus sumatrensis*. Oryx 47 (3), 340–344. https://doi.org/10.1017/S0030605313000045.
Groves, C.P., 1965. Description of a new subspecies of rhinoceros, from Borneo, *Didermocerus sumatrensis harrissoni*. Saeugetierkd. Mitt. 13 (3), 128–131.
Groves, C.P., 1967. On the rhinoceroses of South-east Asia. Saeugetierkd. Mitt. 15 (3), 221–237.
Groves, C.P., 1972. *Ceratotherium simum*. Mamm. Species 8, 1–6. https://doi.org/10.2307/3503966.
Groves, C.P., 1982. The skulls of Asian rhinoceroses: wild and captive. Zoo Biol. 1, 251–261.
Groves, C., 2017. The Sumatran rhino is one-of-a-kind. PACHYDERM 58, 152–153. https://doi.org/10.69649/pachyderm.v58i.430.
Groves, C.P., Kurt, F., 1972. *Dicerorhinus sumatrensis*. Mamm. Species 21, 1–6. https://doi.org/10.2307/3503818.
Groves, C.P., Leslie, D.M., 2011. *Rhinoceros sondaicus* (Perissodactyla: Rhinocerotidae). Mamm. Species 43 (1), 190–208. https://doi.org/10.1644/887.1.
Grue, H., Jensen, B., 1979. Review of the formation of incremental lines in tooth cementum of terrestrial mammals. Dan. Rev. Game Biol. 11 (3), 1–48.
Guérin, C., 1980. Les rhinoceros (Mammalia, Perissodactyla) du Miocene terminal au Pleistocene superieur en Europe occidentale; comparaison avec les especes actuelles. Doc. Lab. Geol. Fac. Sci. Lyon 79, 3–1183.
Hagge, M.D., 2010. A functional and ontogenetic skull analysis of the extant rhinoceroses and *Teleoceras major*, an extinct Miocene north American rhinoceros. LSU Master's Theses 423. https://doi.org/10.31390/gradschool_theses.423.
Havmøller, R.G., Payne, J., Ramono, W.S., Ellis, S., Yoganand, K., Long, B., Dinerstein, E., Williams, A., Putra, R.H., Gawi, J.M., Talukdar, B.K., Burgess, N.D., 2016. Will current conservation responses save the critically endangered Sumatran rhinoceros *Dicerorhinus sumatrensis*? Oryx 50 (2), 355–359. https://doi.org/10.1017/S0030605315000472.
Hieronymus, T.L., Witmer, L.M., Ridgely, R.C., 2006. Structure of white rhinoceros (*Ceratotherium simum*) horn investigated by X-ray computed tomography and histology with implications for growth and external form. J. Morphol. 267 (10), 1172–1176. https://doi.org/10.1002/jmor.10465.
Hillman-Smith, A.K.K., Owen-Smith, N., Anderson, J.L., Hall-Martin, A.J., Selaladi, J.P., 1986. Age estimation of the white rhinoceros (*Ceratotherium simum*). J. Zool. 210 (3), 355–377. https://doi.org/10.1111/j.1469-7998.1986.tb03639.x.
Hillman-Smith, A.K.K., Groves, C.P., 1994. *Diceros bicornis*. Mamm. Species 455, 1–8. https://doi.org/10.2307/3504292.
Hitchins, P.M., 1978. Age determination of the black rhinoceros (*Diceros bicornis* Linn.) in Zululand. S. Afr. J. Wildl. Res. 8 (2), 71–80.
Holbrook, L.T., 2002. The unusual development of the sagittal crest in the Brazilian tapir (*Tapirus terrestris*). J. Zool. 256 (2), 215–219. https://doi.org/10.1017/S0952836902000250.
Howard, B.C., 2016. Rare Sumatran rhino found for first time in 40 years: the female animal is being moved to a more secure location in an attempt to bolster the endangered species. Natl. Geogr. March 25, 2016 https://www.nationalgeographic.com/science/article/160324-sumatran-rhino-borneo-indonesia-kalimantan-endangered-species. (Accessed 13 December 2024).
[ICVGAN] International Committee on Veterinary Gross Anatomical Nomenclature, 2017. Nomina Anatomica Veterinaria, sixth ed. https://www.wava-amav.org/downloads/nav_6_2017.zip.
JASP Team, 2026. JASP (version 0.96.0) [Computer software]. https://jasp-stats.org/.
Kirillova, I.V., Chernova, O.F., van der Made, J., Kukarskih, V.V., Shapiro, B., van der Plicht, J., Shidlovskiy, F.K., Heintzman, P.D., van Kolfschoten, T., Zanina, O.G., 2017. Discovery of the skull of *Stephanorhinus kirchbergensis* (Jäger, 1839) above the Arctic circle. Quat. Res. 88 (3), 537–550. https://doi.org/10.1017/qua.2017.53.
Kirillova, I.V., Shidlovskiy, F.K., 2010. Estimation of individual age and season of death in woolly rhinoceros, *Coelodonta antiquitatis* (Blumenbach, 1799), from Sakha-Yakutia, Russia. Quat. Sci. Rev. 29 (23–24), 3106–3114. https://doi.org/10.1016/j.quascirev.2010.06.036.
Klevezal, G.A., 1995. Recording Structures of Mammals, first ed. Routledge, London. https://doi.org/10.1201/9780203741146.
Lu, X., Deng, T., Pandolfi, L., 2023. Reconstructing the phylogeny of the hornless *Rhinoceros aceratheriinae*. Front. Ecol. Evol. 11, 1005126. https://doi.org/10.3389/fevo.2023.1005126.
Mays Jr., H.L., Hung, C.M., Shaner, P.J., Denvir, J., Justice, M., Yang, S.F., Roth, T.L., Oehler, D.A., Fan, J., Rekulapally, S., Primerano, D.A., 2018. Genomic analysis of demographic history and ecological niche modeling in the endangered Sumatran rhinoceros *Dicerorhinus sumatrensis*. Curr. Biol. 28 (1), 70–76.e4. https://doi.org/10.1016/j.cub.2017.11.021.
Morrow, K.L., Park, R.D., Spurgeon, T.L., Stashak, T.S., Arceneaux, B., 2000. Computed tomographic imaging of the equine head. Vet. Radiol. Ultrasound 41 (6), 491–497. https://doi.org/10.1111/j.1740-8261.2000.tb01876.x.
Moyano, S.R., Giannini, N.P., 2017. Comparative cranial ontogeny of *Tapirus* (Mammalia: Perissodactyla: Tapiridae). J. Anat. 231 (5), 665–682. https://doi.org/10.1111/joa.12666.
Oi, T., 2009. Anthropogenic mortality of Asiatic black bears in two populations in Northern Honshu, Japan. Ursus 20 (1), 22–29. https://doi.org/10.2192/1537-6176-20.1.22.
Pandolfi, L., 2022. A critical overview on early Pleistocene Eurasian *Stephanorhinus* (Mammalia, Rhinocerotidae): implications for taxonomy and paleobiogeography. Quat. Int. 674–675, 109–120. https://doi.org/10.1016/j.quaint.2022.11.008.
Pocock, R.I., 1944. The premaxillae in the Asiatic rhinoceroses. Ann. Mag. Nat. Hist. ser. 11 (11), 834–842.
Preuschoft, H., Witte, H., Witzel, U., 2002. Pneumatized spaces, sinuses and spongy bones in the skulls of primates. Anthropol. Anz. 60 (1), 67–79. https://www.jstor.org/stable/29542345.
Radinsky, L.B., 1966. The families of the Rhinocerotoidea (Mammalia, Perissodactyla). J. Mammal. 47 (4), 631–639. https://doi.org/10.2307/1377893.
Reimers, E., Nordby, Ø., 1968. Relationship between age and tooth cementum layers in Norwegian reindeer. J. Wildl. Manag. 32 (4), 957–961. https://doi.org/10.2307/3799574.
Rookmaaker, L.C., 1984. The taxonomic history of the recent forms of Sumatran rhinoceros (*Dicerorhinus sumatrensis*). J. Malays. Branch R. Asiat. Soc. 57 (1), 12–25. http://www.jstor.org/stable/41492969.
Solounias, N., Fortelius, M., Freeman, P., 1994. Molar wear rates in ruminants: a new approach. Ann. Zool. Fenn. 31 (2), 219–227. http://www.jstor.org/stable/23735376.
Tougard, C., Delefosse, T., Hänni, C., Montgelard, C., 2001. Phylogenetic relationships of the five extant rhinoceros species (Rhinocerotidae, Perissodactyla) based on mitochondrial cytochrome b and 12S rRNA genes. Mol. Phylogenet. Evol. 19 (1), 34–44. https://doi.org/10.1006/mpev.2000.0903.
van Strien, N.J., 1974. *Dicerorhinus sumatrensis* (Fischer): the sumatran or two-horned Asiatic rhinoceros: a study literature. Mededelingen Landbouwhogeschool Wageningen No. 74-16, Veenman, Wageningen 22, 1–82. https://edepot.wur.nl/290944.
Vipin, Sharma, V., Gupta, S.K., Sharma, C.P., Sankar, K., Goyal, S.P., 2018. Development of a fast and low-cost age determination method in spotted deer, *Axis axis*. Folia Zool. 67 (3–4), 186–197. https://doi.org/10.25225/fozo.v67.i3-4.a9.2018.
Wang, H.-B., Bai, B., Gong, Y.-X., Meng, J., Wang, Y.-Q., 2017. Reconstruction of the cranial musculature of the paraceratheriid rhinocerotoid *Pappaceras meiomenus* and inferences of its feeding and chewing habits. Acta Palaeontol. Pol. 62 (2), 259–271. https://doi.org/10.4202/app.00336.2016.
Zeuner, F.E., 1934. Die Beziehungen zwischen Schädelform und Lebensweise bei den rezenten und fossilen Nashornern. Ber. Naturforschenden Ges. Freiburg Breisgau 34, 21–80.